Popular Summary

"Overlap properties of clouds generated by a Cloud Resolving Models"

by L. Oreopoulos[1] and M. Khairoutdinov[2]

Submitted to Journal of Geophysical Research (Atmospheres), December 2002

In order for General Circulation Models (GCMs), one of our most important tools to predict future climate, to correctly describe the propagation of solar and thermal radiation through the cloudy atmosphere a realistic description of the vertical distribution of cloud amount is needed. Actually, one needs not only the cloud amounts at different levels of the atmosphere, but also how these cloud amounts are related, in other words, how they overlap. Currently GCMs make some idealized assumptions about cloud overlap, for example that contiguous cloud layers overlap maximally and non-contiguous cloud layers overlap in a random fashion. Since there are difficulties in obtaining the vertical profile of cloud amount from observations, the realism of the overlap assumptions made in GCMs has not been yet rigorously investigated. Recently however, cloud observations from a relatively new type of ground radar have been used to examine the vertical distribution of cloudiness. These observations suggest that the GCM overlap assumptions are dubious.

Our study uses cloud fields from sophisticated models dedicated to simulate cloud formation, maintenance, and dissipation called "Cloud Resolving Models". These models are generally considered capable of producing realistic three-dimensional representation of cloudiness. Using numerous cloud fields produced by such a CRM we show that the degree of overlap between cloud layers is a function of their separation distance, and is in general described by a combination of the maximum and random overlap assumption, with random overlap dominating as separation distances increase. We show that it is possible to parameterize this behavior in a way that can eventually be incorporated in GCMs. Our results seem to have a significant resemblance to the results from the radar observations despite the completely different nature of the datasets. Ths consistency is encouraging and will promote development of new radiative transfer codes that will estimate the radiation effects of multi-layer cloud fields more accurately.

[1]JCET/University of Maryland Baltimore county
[2]Colorado State University, Fort Collins, CO

Overlap Properties of Clouds Generated by a Cloud Resolving Model

L. Oreopoulos[1,2], and M. Khairoutdinov[3]

Submitted to Geophysical Research Letters

December 2002

1. JCET– University of Maryland Baltimore County, Baltimore, MD

2. Laboratory for Atmospheres, NASA Goddard Space Flight Center, Greenbelt, MD

3. Dept. of Atmospheric Sciences, Colorado State University, Fort Collins, CO

Abstract

The overlap properties of ~850 snapshots of convective cloud fields generated by a Cloud Resolving Model are studied and compared with previously published results based on cloud radar observations. Total cloud fraction is overestimated by the random overlap assumption and underestimated by the maximum overlap assumption, as well as two standard implementations of the combined maximum/random overlap assumption. When the overlap of two layers is examined as a function of vertical separation distance, the value of the parameter a measuring the relative weight of maximum (a=1) and random (a=0) overlap decreases in such a way that only layers less than 1 km apart can be considered maximally overlapped, while layers more than 5 km apart are essentially randomly overlapped. The decrease of a with separation distance is best expressed by a power law; exponential behaviour is, however, still a good approximation for separation distances up to 5 km.

1. Introduction

One of the main requirements for good performance of radiative transfer algorithms of Large Scale Models (LSMs) is input of accurate vertical distributions of cloud fraction (e.g., Barker et al., 1999a). This is, of course, not an easy requirement to meet, since processes relevant to cloud formation that determine cloud area at different levels of the atmosphere are often of subgrid nature and need to be parameterized. Although it is generally accepted that recent progress with prognostic cloud schemes has resulted in improvements in LSM cloudiness, it is still challenging to evaluate the realism of vertical cloud distributions. Moreover, even if input cloud profiles are realistic, it is still doubtful that current operational radiative transfer schemes can incorporate this information in a robust way.

One of the most popular assumptions currently used in LSMs is that adjacent cloud layers overlap maximally while cloud layers separated by clear skies overlap randomly. This is based on a compilation of 15-level US Air Force 3D Nephanalysis data by Tian and Curry (1989). To evaluate the degree of cloud profile realism in LSMs, one needs, however, comparisons with more detailed observations. Unfortunately, there is no such global dataset available to this day. In the future, the space-based 95 GHz radar instrument CLOUDSAT, scheduled to be launched in 2004 will hopefully help in filling this observational gap. But until CLOUDSAT data start becoming available, the best observations of cloud overlap will be ground based and will be coming from millimeter cloud radar (MMCR) operating at few selected sites.

Ground-based radar data have already been used for studies of cloud overlap. Hogan and Illingworth (2000) (hereafter HI2000) derived overlap statistics (discussed later) from radar observations in southern England for the period November 1998 – January 1999. Mace and Benson-Troth (2002) (hereafter MBT2002) performed similar analysis using a much more

extensive data set that included 103 months of MMCR observations at three (tropical, mid-latitude, and polar) sites of the Atmospheric Radiation Measurements (ARM) program and were thus able to examine seasonal cycles in overlap and differences among climate regimes.

In this paper we use a different type of dataset to study overlap: cloud fields from a Cloud Resolving Model (CRM). Cloud fields from CRMs have recently become quite popular inputs for testing atmospheric radiative transfer algorithms (Oreopoulos and Barker, 1999; Barker et al., 1999a; Barker et al., 2002; Scheirer and Macke, 2002; Di Giuseppe and Tompkins, 2002). The rationale for their use in this role, is that they are the most realistic 3D representation of cloud fields that is presently available. Furthermore, they provide instantaneous full 3-D "snapshots" of clouds with well-defined spatial scales, in contrast to cloud fields reconstructed from MMCR *point* observations that are, at best, 2D, and this only after having to invoke the frozen turbulence assumption (MBT2002). In this work, we proceed then with the assumption that the realism of CRM cloud fields justifies their use as a source of useful statistical information on the vertical overlap of clouds. It should be pointed out, however, that our results should be considered representative of convective clouds only, and are specific to the vertical bin size used in our analysis (0.5 km), the horizontal (2 km) resolution, and the size of the domain (~500 km).

2. The dataset

A detailed description of the CRM used in this study is given by Khairoutdinov and Randall (2002). The convective cloud fields come from runs using the time varying forcing derived from the observations collected during intensive observation periods (IOPs) of ARM, GATE[1], and TOGA-COARE[2]. The ARM forcing is from the Summer 1997 IOP over Oklahoma and

[1] Global Atmospheric Research Program (GARP) Atlantic Tropical Experiment
[2] Tropical Ocean and Global Atmosphere Coupled Ocean-Atmosphere Response Experiment

Nebraska from 18 June to 16 July; the GATE Phase III forcing covers the period from 1 to 18 September 1974; finally, the TOGA-COARE (hereafter, for brevity, "TOGA") dataset corresponds to the time period from 18 December 1992 to 8 January 1993. For all three cases, the domain size is 512 km x 512 km with 2km horizontal grid size and variable vertical resolution: ~100-200 m up to the first two kilometers, gradually increasing to 500 m at a height of ~ 6km. The number of fields produced from the runs with significant amount of clouds for statistical analysis is 193 for ARM, 160 for GATE, and 498 for TOGA and are "snapshots" saved at hourly intervals. For each model layer the cloud fraction is determined by counting the number of gridboxes with non-precipitating total water (liquid and ice) greater that 10^{-5} g/Kg. Figure 1 shows cloud fraction and liquid water content (LWC) profiles derived by ensemble-averaging individual cloud fields. GATE fields have larger cloud fractions than the ARM and TOGA fields, except for high altitudes where TOGA has slightly more clouds. TOGA has the highest LWC at low altitudes (< 4 km) where the cloud fractions are very low, and ARM the the highest above that altitude. Even though no layer of the GATE and TOGA dataset has ensemble-average cloud fraction above 0.5, the total cloud fraction (fraction of columns with at least one cloudy gridbox) as viewed from above, is much higher (mean values of "true" curve in Fig. 2b,c), and frequently assumes values corresponding to overcast conditions.

3. Overlap analysis

The large number of cloud fields from the CRM runs gives us some assurance that meaningful statistics on the overlap characteristics of clouds can be obtained. As we go through the presentation of our results, we will be providing information on how to calculate cloud fractions

from the various overlap assumptions. We start immediately below with three classic overlap assumptions.

Given two cloud layers, their combined cloud fraction, when only their individual cloud fractions C_1 and C_2 are known, can be calculated from one of the three standard overlap assumptions (e.g. MBT2002):

$$C_{max} = \max(C_1, C_2) \quad (1a)$$

$$C_{min} = \max(1, C_1 + C_2) \quad (1b)$$

$$C_{rand} = C_1 + C_2 - C_1 C_2 \quad (1c)$$

which are, respectively, the cloud fractions corresponding to the maximum, minimum, and random overlap assumption. The true combined cloud fraction of two cloud layers most often does not agree with any of the cloud fractions derived from (1). HI2000 introduced a parameter a to quantify the degree of agreement between the combined true cloud fraction C_{true} and that from the overlap assumptions:

$$C_{true} = a\, C_{max} + (1 - a)\, C_{rand} \quad (2)$$

According to the above formulation, $a = 0$ corresponds to random overlap, $a = 1$ to maximum overlap, while negative values of a indicate cloud fractions larger than C_{rand} that start approaching values of C_{min}.

Figure 2 shows the total cloud fraction for each cloud field. Five different estimates are shown. "True" is the actual total cloud fraction, as "observed". It is estimated as the fraction of

the total number of columns that are cloudy. A column is considered cloudy if it contains one or more cloudy gridboxes. The "max" curve corresponds to the total cloud fraction using the maximum overlap assumption (generalization of eq. 1a for multiple cloud layers) and is simply equal to the maximum cloud fraction of the vertical profile. The "ran" curve corresponds to the total cloud fraction from the random overlap assumption and is derived from a generalization of eq. (1c) for multiple (N) cloud layers:

$$C_{ran} = 1 - \prod_{i=1}^{N}(1 - C_i) \qquad (3)$$

The "maxran blocks" curve is derived by combining the maximum and random overlap assumption in the following way: contiguous cloud layers form blocks. Whenever a clear layer is present a new cloud block is formed; the cloudy layers within a block overlap according to the maximum overlap assumption, while cloud blocks themselves overlap according to the random overlap assumption. Thus, eq. (3) is used with N as the number of cloud blocks and each C_i represents the maximum cloud fraction within the block. Finally, the curve "maxran GH" is the total cloud fraction according to the combined maximum/random overlap assumption as implemented by Geleyn and Hollingsworth (1979):

$$C_{\text{maxran}} = 1 - (1 - C_1) \times \prod_{i=2}^{N} \frac{1 - \max(C_{i-1}, C_i)}{1 - C_{i-1}} \qquad (4)$$

The Geleyn and Hollingsworth (1979) implementation of maximum/random overlap differs from the "block" approach in that layers within a block are considered maximally overlapped only

when there is no local cloud minimum in between. Thus, the Geleyn and Hollingsworth method generally results in a larger cloud fraction than the "block" method.

For the CRM fields, the true total cloud fraction assumes values between those derived from the random and maximum overlap assumptions. In addition, neither of the two max/ran overlap assumptions is a particularly good fit. The "block" max/ran scheme gives values almost identical to the maximum overlap scheme for all three sets of runs. The reason is that in the vast majority of fields, clouds form a single block, i.e., clouds are contiguous. For the GATE fields, eq. (4) performs better than the maximum overlap assumption, but still underestimates substantially the true cloud fraction.

Figure 3 shows the values of a derived from eq. (2) with input for C_{true}, C_{max} and C_{rand} taken from the data used to draw the "true", "max", and "ran" curves in Fig. 2. Clearly, the ARM cloud fields exhibit much stronger resemblance to maximum overlap than the GATE and TOGA cloud fields. The cases where a approaches zero for GATE and TOGA corresponds to nearly overcast conditions. In general, a and C_{true} are well correlated for all three datasets with small values of a corresponding to large values of C_{true} and vice-versa.

Figure 4 shows the combined cloud fraction of two cloudy layers as a function of their vertical separation distance shown in the ordinate. The true combined cloud cover is compared with combined cloud cover derived from the maximum, random, and minimum overlap assumptions. The vertical separation bin size is 500 m. This figure is similar to Fig. 3 of HI2000 and the (a) panels of Fig. 3-5 in MBT2002. Note, however, that in contrast to their work, we do not distinguish between pairs of layers with and without cloud in the intervening layers. The reason is that in the vast majority of cases only one cloud block is present (recall the small difference between "max" and "maxran blocks" cloud fraction in Fig. 2), so that statistics for the

rare occurences of layers separated by clear skies are quite limited and applicable only to the case of large separation distances. As expected, the true combined cloud fraction of the pair lies between its counterparts for the random and maximum overlap assumption. For small separation distances (first two bins, < 1000 m) the two layers overlap in a manner resembling maximum overlap conditions, but very quickly the overlap takes values between those for maximum and random overlap. Conditions of almost purely random overlap prevail when the layers are separated by more than 5 km. For radiative transfer calculations, however, it would probably not be wise to attempt to incorporate overlap effects of clouds separated by large distances, unless, of course, only clear skies exist between the two distant layers. When some of the intervening layers are cloudy, radiative interactions are already so complex that the detailed overlap of two remote layers will at most times have minimal effect on the radiative fluxes.

Figure 5 shows profiles of a derived from eq. (2) using pairs of cloud layers separated by a range of distances. There are two curves for each of the ARM, GATE, and TOGA cloud fields: one by inserting in eq. (2) the ensemble values of C_{true}, C_{max} and C_{rand} shown in Fig. 4, and one by taking the ensemble average of a profiles derived for each individual cloud field. Both methods for estimating a profiles yield very similar results for ARM and GATE, but non-negligible differences above ~ 2 km for TOGA. As expected, a drops with separation distance, indicating that as cloud layers become more distant they acquire an increasingly stronger tendency for random overlap.

Figure 6 shows least-square fits to the ensemble average a curves of Fig. 6. It is interesting that better fits over the entire range of separation distance Δz are obtained with power law functions

$$a = c\Delta z^{-b} \qquad (5a)$$

than exponential functions

$$a = \gamma \exp(-\beta \Delta z) \qquad (5b)$$

as in HI2000. The fitted values of c, b, as well as the correlation coefficient R for each of the three datasets is provided in Table 1. The least successful power law fit is for the TOGA dataset. When the fits are restricted to a maximum of 5 km separation distances, a for TOGA follows almost perfectly (R=0.996) an exponential drop; for the other two datasets exponential and power fits perform about equally well. We show the exponential fit curves for separation distances up to 5 km in the bottom panel of Fig. 6, and the least square values for γ, β, and R in Table 2.

Provided that fits of this type can be reproduced from other datasets, one can envision the introduction in an LSM of a completely generalized overlap scheme where the combined cloud fraction of any two layers is given by eq. (2) with a values provided as a function of separation distance from parameterizations such as eq. (5). A solar radiative transfer algorithm applying these ideas was presented by Bergman and Rasch (2002).

4. Discussion and conclusions

We have shown that the overlap properties of numerous convective cloud fields generated by a CRM show some consistency with previous analyses from ground-based millimeter radar data (HI2000; MBT2002). We reach this conclusion using the spatial cloud variability and without attempting to emulate MMCR-type cloud observations with the time series of our CRM

"snapshots" as in Barker et al. (1999b) because of the coarse temporal sampling (1 hour). We found that the total cloud fraction and the combined cloud fraction of any two layers separated by a certain distance assumes values between those corresponding to the commonly used maximum and random overlap assumptions. The value of the parameter a describing the degree to which cloud fraction agrees with one of the two idealized overlap assumptions is a smooth varying function of separation distance and can be fit with analytical functions. This may turn out to be very useful for parameterization purposes..

Overlap information such as this presented in the current study should continuously be extended with results for other cloud types and ultimately be incorporated in the radiative transfer schemes of LSMs or even stochastic multi-layer cloud generators. Efforrts have already begun in this direction (Bergman and Rasch 2002; Oreopoulos et al., 2002), despite the inherent difficulties in conveying the overlap information into the radiation algorithm in a meaningful way. Things become even more complex when attempting to simoultaneously account for cloud overlap, horizontal inhomogeneity, and vertical correlations of cloud water. Nevertheless, initial evidence suggests that even at their current stage of development these algorithms outperform current plane-parallel algorithms with standard overlap assumptions.

Acknowledgements This research was supported by the Office of Biological and Environmental Research of the U. S. Department of Energy (under grant DE-AI02-00ER62939) as part of the Atmospheric Radiation Measurement Program, and NASA grant NAG5-11631. We benefited from discussions with H. W. Barker and P. Räisänen.

References

Barker, H. W., G. L. Stephens, and Q. Fu, The sensitivity of domain-averaged solar fluxes to assumptions about cloud geometry, *Quart. J. Roy. Meteor. Soc.*, *125*, 2127-2152, 1999a.

Barker, H. W., E. E. Clothiaux, T. P. Ackerman, R. T. Marchand, Z. Li, and Q. Fu, Overlapping cloud: What radars give and what models require, 9th ARM Science Team Meet. Proc., http://www.arm.gov/docs/documents/technical/conf_9903/barker-99.pdf, 1999b.

Barker, H. W., and 31 coauthors, Assessing 1D atmospheric solar radiative transfer models: interpretation and handling of unresolved clouds, *J. Climate*, submitted, 2002.

Bergman, J. W., and P. J. Rasch, Parameterizing vertically coherent cloud distributions, *J. Atmos. Sci.*, *59*, 2165-2182, 2002.

Di Giuseppe, F., and A. M. Tompkins, Three dimensional radiative transfer in tropical deep convective clouds, *J. Atmos. Sci.*, submitted, 2002.

Geleyn, J. F., and A. Hollingsworth, An economical analytical method for the computation of the interaction between scattering and line absorption of radiation, *Contrib. Atmos. Phys.*, *52*, 1-16, 1979.

Hogan, R. J., and A. J. Illingworth, Deriving cloud overlap statistics from radar, *Q. J. R. Meteor. Soc.*, *126*, 2903-2909, 2000.

Khairoutdinov, M. F., and D. A. Randall, Cloud resolving modeling of the ARM Summer 1997 IOP: Model formulation, results, uncertainties and sensitivities, *J. Atmos. Sci.*, in press, 2002.

Mace, G. G., and S. Benson-Troth, Cloud layer overlap characteristics derived from long-term cloud radar data, *J. Climate*, *15*, 2505-2515, 2002.

Oreopoulos, L., and H. W. Barker, Accounting for subgrid-scale cloud variability in a multi-

layer 1D solar radiative transfer algorithm, *Quart. J. Roy. Meteor. Soc.*, *126*, 301-330, 1999.

Oreopoulos, L., H. W. Barker. M.-D. Chou, R. F. Cahalan, and M. Khairoutdinov, Allowing for inhomogeneous clouds in the Goddard Earth Observing System GCM Column Radiation Model, *Proc. of 11th Conf. on Atmospheric Radiation*, Ogden, Utah, J185-J187, 2002.

Scheirer, R., and A. Macke, Cloud inhomogeneity and broadband solar fluxes, *J. Geophys. Res.*, submitted, 2002.

Tian, L. and J. A. Curry, Cloud overlap statistics, *J. Geophys. Res.*, *94*, 9925-9935, 1989

List of Tables

Table 1

Least square fits and correlation coefficient for eq. (5a).

	c	b	R
ARM	56.1	-0.65	0.944
GATE	78.3	-0.75	0.970
TOGA	299.1	-0.93	0.906

Table 2

Least square fits and correlation coefficient for eq. (5b).

	γ	β	R
ARM	0.836	2.81×10^{-4}	0.961
GATE	0.773	4.30×10^{-4}	0.966
TOGA	0.959	4.69×10^{-4}	0.996

List of figures

Figure 1 Ensemble average profiles of cloud fraction and liquid water content for the simulated ARM, GATE and TOGA cloud fields used in this study.

Figure 2 Total cloud fraction of each cloud field used in this study as estimated exactly from the number of cloudy gridboxes ("true") and as calculated from layer cloud fractions using the random ("ran"), maximum ("max") and two maximum/random overlap assumptions ("maxran blocks" and "maxran GH"). See text for details.

Figure 3 Alpha parameter values corresponding to total cloud fraction for each of the ARM, GATE, and TOGA cloud fields.

Figure 4 Combined cloud fraction of pairs of layers separated vertically by distances shown in the ordinate as "observed" from the modeled fields ("true"), and as derived using the maximum ("max"), random ("ran"), and minimum ("min") overlap assumptions.

Figure 5 Profiles of alpha derived by either ensemble-averaging the alpha profiles of each individual cloud field (dotted curves) or by applying eq. (2) to the ensemble average of combined cloud fractions shown in Fig. 4 (solid curves). Thin black curves are for ARM, thick black curves for GATE and gray curves for TOGA.

Figure 6 Ensemble average alpha profiles as a function of distance (black curves), as in Fig. 5, but with the axes swapped, power law least square fit curves (gray curves) up to separation distances of 15 km (top panel), and exponential fits up to separation distances of 5 km (bottom panel).

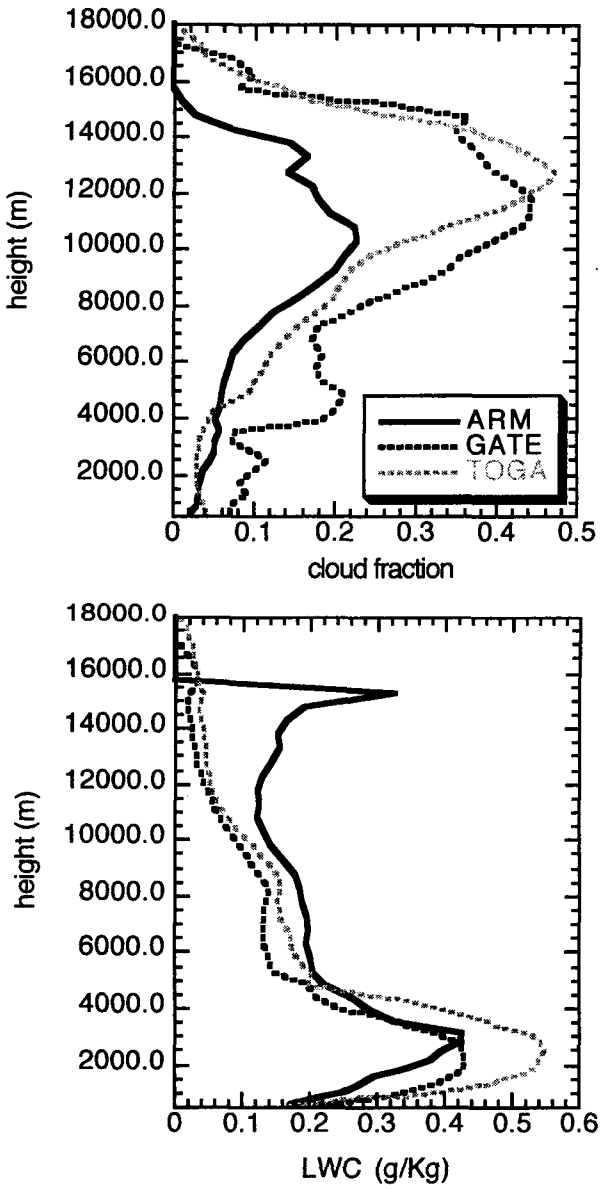

Figure 1 Ensemble average profiles of cloud fraction and liquid water content LWC for the simulated ARM, GATE and TOGA cloud fields used in this study.

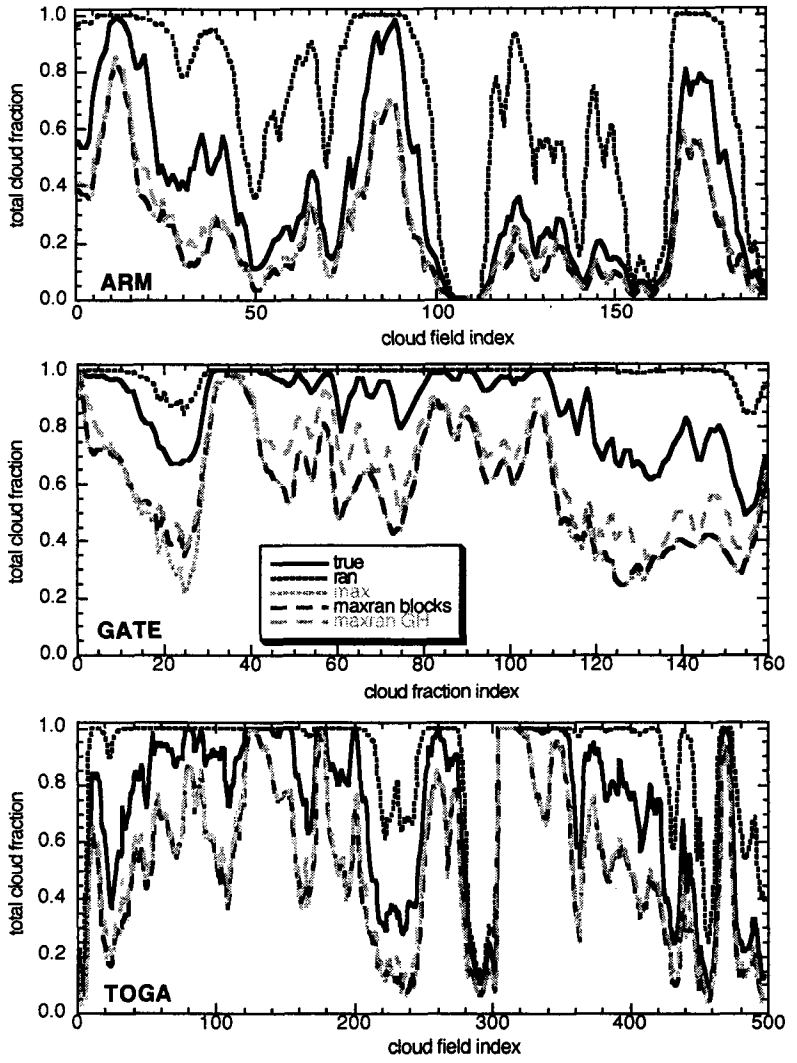

Figure 2 Total cloud fraction of each cloud field used in this study as estimated exactly from the number of cloudy gridboxes ("true") and as calculated from layer cloud fractions using the random ("ran"), maximum ("max") and two maximum/random overlap assumptions ("maxran blocks" and "maxran GH"). See text for details.

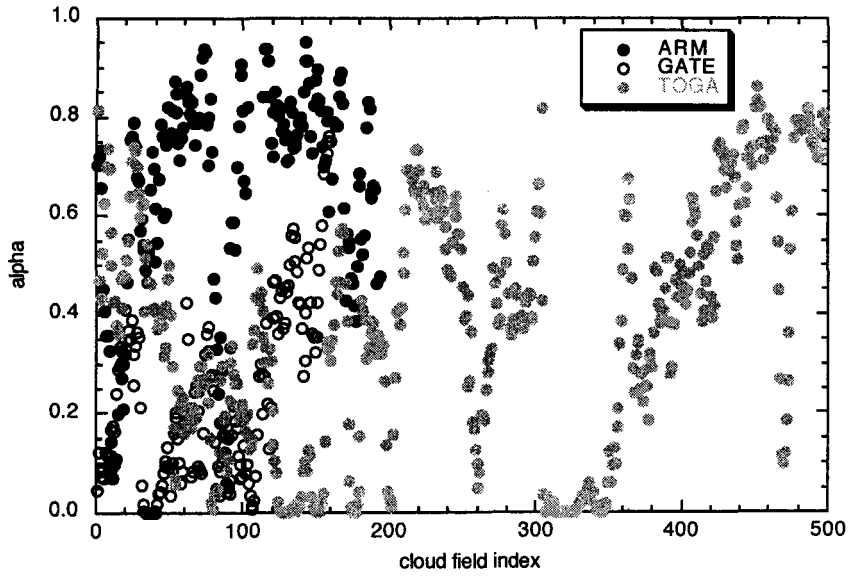

Figure 3 Alpha parameter values corresponding to total cloud fraction for each of the ARM, GATE, and TOGA cloud fields.

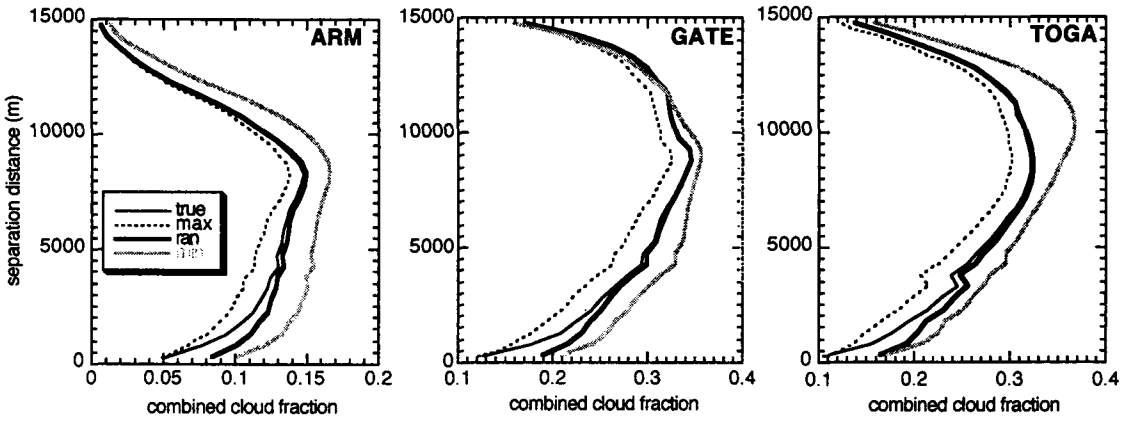

Figure 4 Combined cloud fraction of pairs of layers separated vertically by distances shown in the ordinate as "observed" from the modeled fields ("true"), and as derived using the maximum ("max"), random ("ran"), and minimum ("min") overlap assumptions.

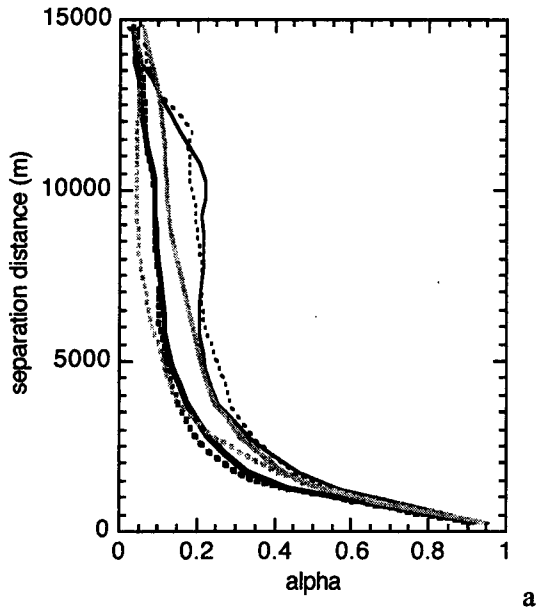

Figure 5 Profiles of alpha derived by either ensemble-averaging the alpha profiles of each individual cloud field (dotted curves) or by applying eq. (2) to the ensemble average of combined cloud fractions shown in Fig. 4 (solid curves). Thin black curves are for ARM, thick black curves for GATE and gray curves for TOGA.

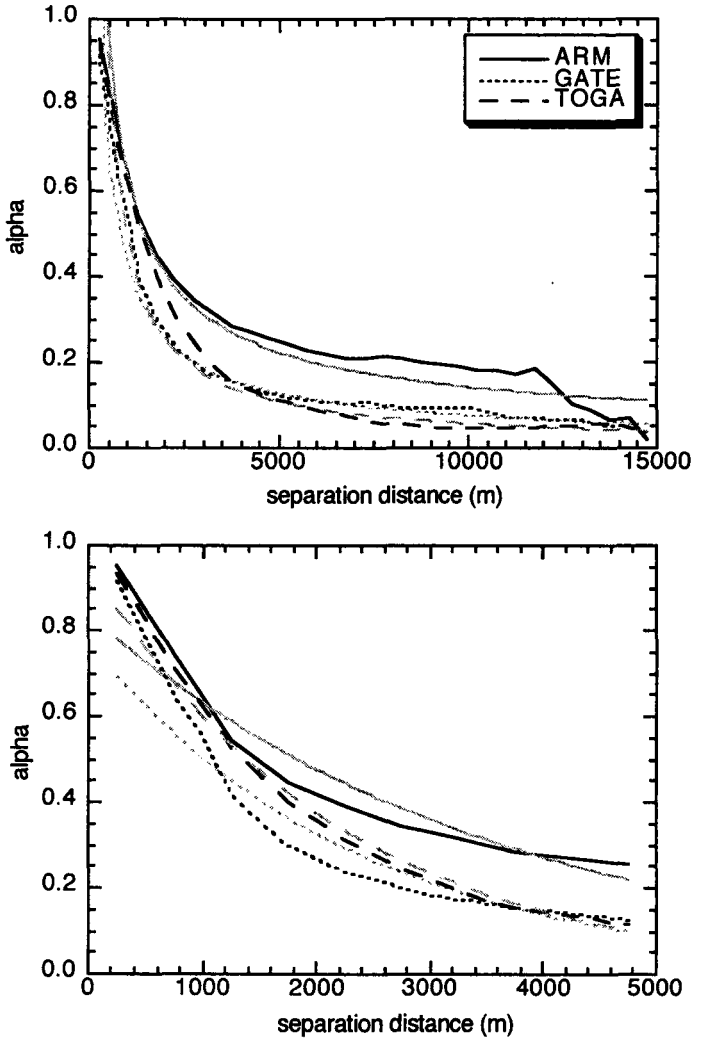

Figure 6 Ensemble average alpha profiles as a function of distance (black curves), as in Fig. 5, but with the axes swapped, power law least square fit curves (gray curves) up to separation distances of 15 km (top panel), and exponential fits up to separation distances of 5 km (bottom panel).